Harnessing Quantum Interference in Molecular Dielectric Materials

Justin P. Bergfield,*,† Henry M. Heitzer,† Colin Van Dyck,† Tobin J. Marks,*,† and Mark A. Ratner*,†

†Department of Chemistry and the Materials Research Center, Northwestern University, 2145 Sheridan Road, Evanston, Illinois 60208, United States

ABSTRACT We investigate the relationship between dielectric response and charge transport in molecule-based materials operating in the quantum coherent regime. We find that quantum interference affects these observables differently, for instance, allowing current passing through certain materials to be reduced by orders of magnitude without affecting dielectric behavior (or band gap). As an example, we utilize *ab initio* electronic structure theory to calculate conductance and dielectric constants of cross-conjugated anthraquinone (AQ)-based and linearly conjugated anthracene (AC)-based materials. In spite of having nearly equal fundamental gaps, electrode bonding configurations, and molecular dimensions, we find a ∼1.7 order of magnitude (∼50-fold) reduction in the conductance of the AQ-based material relative to the AC-based material, a value in close agreement with recent measurements, while the calculated dielectric constants of both materials are nearly identical. From these findings, we propose two molecular materials in which quantum interference is used to reduce leakage currents across a ∼25 Å monolayer gap with dielectric constants larger than 4.5.

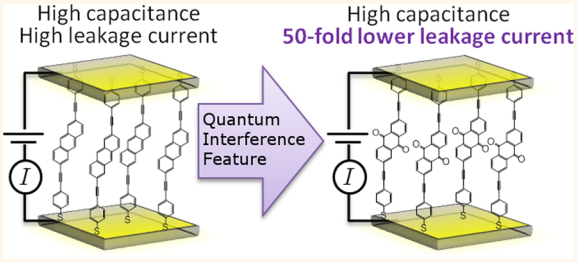

KEYWORDS: molecular dielectric material · quantum interference · density functional theory · nonequilibrium quantum transport · cross-conjugated polymers

High dielectric constant materials which exhibit low leakage currents are desirable, for instance, to ensure the continued Moore's law-like increase in microprocessor transistor density without a commensurate increase in power consumption.[1] Molecule-based dielectric materials are particularly attractive since their response can in principle be tailored to support either high- or low-dielectric applications, and they can be integrated into existing organic electronic devices.[2−4] The fundamental gap of many small organic molecules is on the order of several electron volts, meaning that molecular materials can be designed with low leakage currents (*e.g.*, a monolayer of long saturated molecular strands). However, the low-frequency dielectric response of many bulk semiconductors is inversely proportional to the band gap energy, where a large band gap corresponds to strongly bound electrons which are only weakly polarizable by an external electric field.[5−8] This means that long saturated chains will exhibit low dielectric (and capacitance) values, and that any high-dielectric response molecular material must necessarily be conjugated and therefore exhibit a substantial leakage current, apparently limiting the technological applicability of organic dielectrics.

In the coherent transport regime, the current flow often depends critically on both the energetics and symmetries of the states involved. Quantum interference effects are ubiquitous in small organic molecules and are often robust even at room temperature,[9,10] where characteristic electron−phonon coupling and thermal energies are typically much less than the electrode−molecule bonding energies. In these systems, current through electrodes bridged by a molecular wire often depends critically on the wave-like mixing and interferences between numerous transport paths, which in turn depend on the details of molecular structure, molecule−electrode bonding, and the dispersion of the electrodes.[11−17] Recently, direct experimental evidence of (destructive) quantum interference was observed in the low-temperature differential conductance of a molecular self-assembled monolayer (SAM) material.[18] Although interference effects on charge transport have been studied extensively both theoretically[12−14,17,19−23] and experimentally,[16,18,24] the dielectric response of molecular materials operating in the quantum limit has received relatively little attention.

* Address correspondence to justin.bergfield@northwestern.edu, t-marks@northwestern.edu, ratner@northwestern.edu.

Received for review April 6, 2015 and accepted May 26, 2015.

Published online May 26, 2015
10.1021/acsnano.5b02042

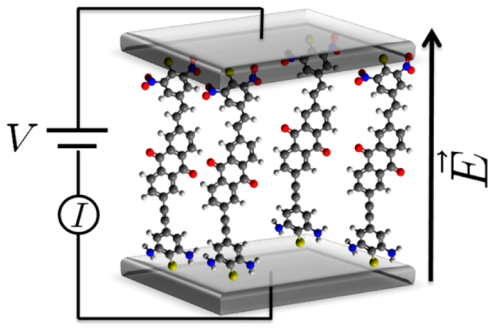

Figure 1. Schematic representation of the molecular devices considered here, composed of a single layer of molecules sandwiched between two metallic electrodes. We investigate the relationship between the conductance *G*, which is the proportionality coefficient between the applied voltage *V* and the current *I*, and the dielectric function ε, which is the ratio between an external and the total potential and is related to the polarizability of the charge density.

In this contribution, we investigate the theoretical connection between dielectric response and transport in the coherent regime. As an example, we consider the response of two SAM-based materials (shown schematically in Figure 1) where the effects of quantum interference can be unambiguously identified. On the basis of these findings, we propose two materials in which the dielectric response is large while the current is simultaneously minimized *via* destructive interference.

THEORY

To help elucidate the connection between dielectric response and transport, we consider a material system operating in linear-response, where the effects of an applied field may be treated perturbatively. In this regime, the fluctuation−dissipation theorem (FD) can be used to relate nonequilibrium response functions to equilibrium fluctuations.[25−27] In particular, dielectric response and conductivity may be expressed in terms of density−density and current−current correlations, respectively. Without approximation, the dielectric function may be written as[26,28]

$$\varepsilon^{-1}(\omega) = \mathbf{1} - U\Pi(\omega) \tag{1.1}$$

where U is the bare (*i.e.*, instantaneous) Coulomb potential matrix, and Π is the polarizability—the response of the density to an external potential. The representation of these functions in a given basis is implied. With the use of the FD theorem, the polarizability may be expressed as[26,27]

$$\Pi_{nm}(\omega) = -i\int_0^\infty \mathrm{d}t e^{i\omega t}\langle[\hat{\rho}_n(t), \hat{\rho}_m(0)]\rangle \tag{1.2}$$

where angular brackets denote the canonical ensemble average using the equilibrium density matrix, and *m* and *n* are basis indices. Similarly, the FD theorem may be applied to find the Kubo formula for the conductivity,[26,29]

$$\sigma_{nm}(\omega) = i\frac{e^2 n_0}{m\omega}\delta_{nm} + \frac{1}{\omega\hbar\nu}\int_0^\infty \mathrm{d}t e^{i\omega t}\langle[\hat{I}_n^\dagger(t), \hat{I}_m(0)]\rangle \tag{1.3}$$

where the first (diamagnetic) term is expressed in terms of the equilibrium charge density n_0, the electron mass m, and the electron charge e, and the second term is averaged over the volume ν, and $\hat{I}_n = \sum_{i,j} p_n^{(ij)} \hat{d}_i^\dagger \hat{d}_j$ is the current operator with electronic creation operator † with matrix elements $p_n^{(ij)}$.

Although it is tempting to equate the current to the time-derivative of the charge-density in the equations above, the density−density and current−current correlation functions do not factorize for a general interacting nanostructure, meaning that the relative phases of off-diagonal terms are likely to play an important role. This is especially true in the small organic systems considered here, which form covalent bonds with the electrode and in which transport is predominantly coherent and elastic, even with a moderate bias applied at room temperature.[9,10,24] Equations 1.1−1.3 also indicate that structure−function relationships for dielectric response and transport differ in quantum coherent systems, since the density and current do not often depend on bonding configurations, molecular symmetries, and energy level alignments in the same way.

These points can be further clarified by utilizing the scattering approach to transport,[30,31] in which elastic quantum coherent transport is described in terms of electronic transmission amplitudes. At the nanoscale, it is generally appropriate to consider the conductance rather than conductivity, which may be expressed in terms of the transmission amplitudes $t(E)$ as[25]

$$\frac{\mathrm{d}I}{\mathrm{d}V} = G_0\int \mathrm{d}E\left(-\frac{\partial f_0}{\partial E}\right)Tr\{t(E)t^\dagger(E)\} \tag{1.4}$$

where f_0 is the Fermi−Dirac distribution for the electrodes in equilibrium, and $G_0 = 2e^2/h$ is the conductance quantum. The transmission amplitude for scattering from electrode β to electrode α for electrons with energy E is given by[15,32]

$$t(E) = i\gamma_\alpha(E)G(E)\gamma_\beta^\dagger(E) \tag{1.5}$$

where the electrode−molecule bonding is described by the tunneling-width amplitude matrices $\gamma(E)$, and the propagation of electronic excitations is described by the junction's retarded Green's function $G(E)$. Additional details are given in the Methods section.

As described by eq 1.4, conductance is related to the modulus squared of the transmission amplitudes. Conversely, the dielectric response is related to the density of states which is related to the transmission amplitude phases and their derivatives *via* the Friedel sum-rule.[33−35] At finite frequency, the phase

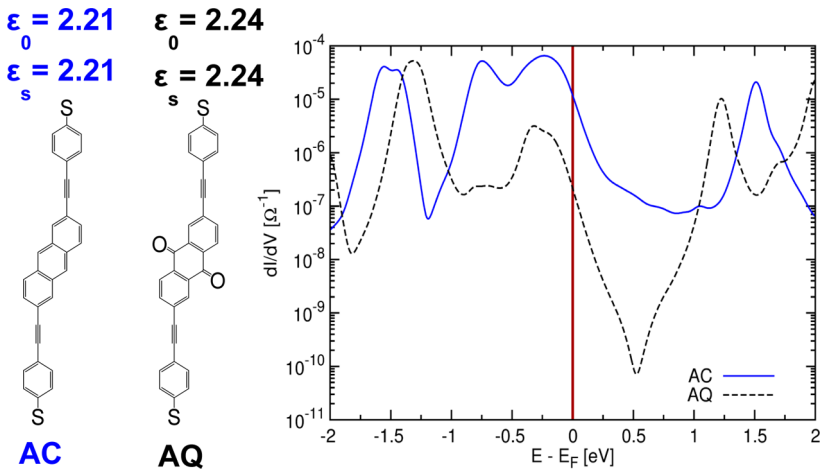

Figure 2. Calculated dielectric constants ε_s, ε_0, and single-molecule conductance d*I*/d*V* of anthracene-based (AC) and anthraquinone-based (AQ) molecular monolayer materials sandwiched between Au electrodes. In the vicinity of the Au Fermi energy E_F (red vertical line), the conductance of the AQ and AC junctions are 0.21 and 11.4 μS, respectively. The origin of the ∼1.7 order of magnitude (∼50-fold) drop in the AQ material's conductance, a value in close agreement with recent measurements of the same systems,[18] is destructive quantum interference. In contrast, the optical and static dielectric constants for these materials are nearly identical $\varepsilon_0 \approx \varepsilon_s \approx 2.2$. All calculations are for junctions operating in linear response at 300 K.

and amplitude of the transmission are typically related *via* the usual Kramer−Kronig relationships. However, for low frequencies, these two aspects can be essentially independent. Motivated by these observations, we consider the influence of quantum interference on the transport and dielectric response of several molecular-based materials.

RESULTS AND DISCUSSION

The Influence of Quantum Interference. We first consider materials composed of monolayers of either linearly conjugated anthracene-based (AC) molecules or cross-conjugated anthraquinone-based (AQ) molecules sandwiched between Au electrodes. A schematic representation of the material and the chemical structures of each molecule are shown in Figure 1, and the left-hand portion of Figure 2, respectively.

Linear conjugation refers to a sequence of alternating single and double bonds between the termini of a molecule, while cross-conjugation refers to the fact that the sequence of alternating single and double bonds has been interrupted.[36,37] In both cases, all carbon atoms are sp^2 or sp hybridized, ensuring an itinerant electronic system which dominates the electronic transport. Recently, direct experimental evidence of a destructive quantum interference feature (a node) was observed in the low-temperature conductance spectrum of AQ-based materials, while no such feature was observed in the corresponding AC-based materials.[18] The node's origin can be understood in terms of eq 1.4, where at low temperatures and low biases, d*I*/d*V* ∼ $G_0 Tr(tt^{\dagger})$, and the transmission amplitudes are evaluated at the electrode Fermi energy. The carbonyl side groups in the AQ molecule introduce transmission amplitudes, which, for electrons with energy $E - E_F \sim 0.5$ eV, cause a complete cancellation in the total charge transport through the π-system at that energy at zero temperature.[12,13] Aside from this difference, the AQ and AC molecules have remarkably similar material properties, making them ideal for our comparison. Specifically, both molecules have lengths ∼24.5 Å, bond to Au electrodes *via* thiol terminating groups, and exhibit energy gaps between their highest occupied molecular orbital (HOMO) and lowest unoccupied molecular orbital (LUMO) of 2.90 and 2.88 eV, respectively.[28] We emphasize that this is an example system. Nodes are a generic feature of coherence and have been predicted in a variety cross-conjugated[12,20,38] and linearly conjugated[11,13,14,17,19,21,39] molecular systems.

Calculated room-temperature conductance spectra for single-molecule Au−AQ−Au and Au−AC−Au junctions are shown in Figure 2. In the vicinity of the electrode Fermi energy, the AC and AQ devices exhibit conductance values of 11.4 and 0.21 μS, respectively, a reduction ratio in close agreement with low-temperature measurements on the same systems.[18] In contrast, we find that the computed optical and static dielectric constants (ε_0 and ε_s, respectively) of these materials are virtually indistinguishable, giving ∼2.24 for the AQ material and ∼2.21 for the AC material. The transmission spectra were calculated using nonequilibrium Green's functions (NEGF) in conjunction with Kohn−Sham density functional theory (KS-DFT), using a pseudopotential approach and assuming the elastic quantum limit. We consider symmetric junctions for molecules bonded to Au(111) with an Au−S distance of 2.42 Å, and the room-temperature conductance was calculated using eq 1.4. The dielectric constant of each monolayer film was calculated using a finite difference approach in conjunction with KS-DFT,[3]

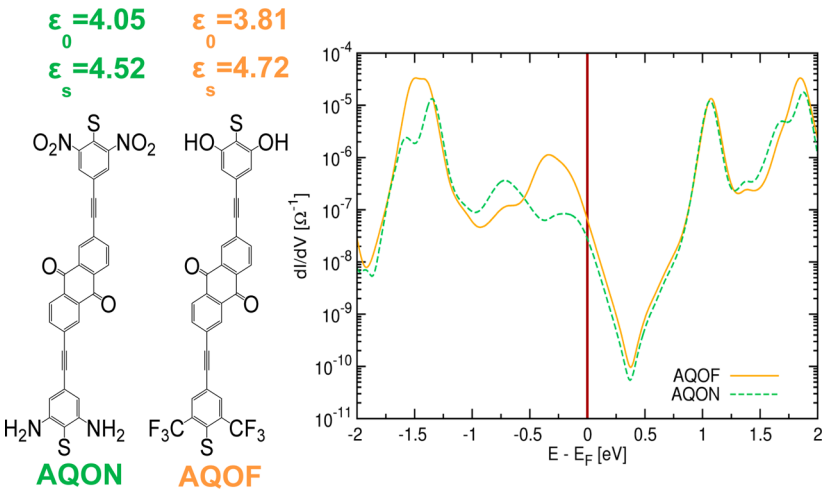

Figure 3. Calculated dielectric constants ε_s, ε_0 and single-molecule conductance d*I*/d*V* of Au−AQON−Au and Au−AQOF−Au molecular monolayer sandwiches. The donor−acceptor substituents enhance the dielectric constant but do not eliminate the transmission node ($E - E_F \sim 0.35$ eV) and associated reduction in conductance. In the vicinity of the Au Fermi energy E_F (red vertical line), the AQON and AQOF materials exhibit conductance values of 27.8 and 64.9 nS, corresponding to a conduction reduction relative to the AC material of ~2.6 and ~2.3 orders of magnitude, respectively. All calculations are for junctions operating in linear response at 300 K.

with a surface coverage of 2.5 molecules/nm^2 and an external electric field applied along the *z*-axis. Additional details of our computational techniques are discussed in the Methods section.

Contrary to trends expected from classical bulk semiconductors,[8] the gap and dielectric constants of AC and AQ materials are nearly identical, while the current is reduced by ~1.7 orders of magnitude (*i.e.*, ~50-fold decrease). Although the bulk dielectric response and conductivity may often be formulated in terms of one another,[26] in systems without 3-dimensional translational invariance, such as the molecular materials considered here, off-diagonal elements contribute, making the mathematical relationship between these observables complex and indirect (*cf.*, eqs 1.1−1.3). Physically, the similar dielectric responses of the AQ and AC materials can be understood in terms of the additive nature of the total displacement current and polarizability, where the broken conjugation in the AQ molecule has a negligible effect on the local response of the charge-density.

Assuming negligible molecular cross-talk and the same surface coverage used in the dielectric calculations, the computed current densities through AC and AQ-based monolayer materials are 10.5 and 0.24 μA/nm^2 at 0.25 V (corresponding to ~1 MV/cm), respectively. Note that these molecules were selected to highlight the utility of quantum interference in dielectric material design, not to minimize leakage current. For a particular application, the current should be tunable by changing the surface coverage, or electrode material, or by employing a variety of molecular design principles. For instance, leakage currents may be reduced by orders of magnitude by increasing the length of the molecule, breaking the electrode−molecule bonding symmetry, selecting molecules with larger gap energies, or tuning the electrode−molecule level alignment.[12,40,41]

High Dielectric Material Design. The above AQ and AC system calculations show that a high-dielectric material may be designed in which leakage current is reduced *via* quantum interference. Materials with large (hyper)polarizabilities possess significantly higher dielectric responses than typical organic materials, while donor and acceptor moieties are known to enhance molecular (hyper)polarizabilities when added in tandem to conjugated organics. These molecules, commonly referred to as Donor-Bridge-Acceptors (DBAs), have inspired significant research in the scientific community for applications in nonlinear optics,[42,43] charge transfer, and charge transport.[44,45]

Here, we propose two DBA molecules designed to simultaneously exhibit large dielectric responses and a transmission node: AQON and AQOF, which are AQ with NH_2−NO_2 and OH−CF_3 donor−acceptor substituent combinations, respectively. The chemical structure, calculated dielectric response, and conductance spectra of these molecules are shown in Figure 3. Owing to the substituted groups, dielectric constants of both molecules are enhanced compared to the AQ material ($\varepsilon_0 = 4.05$, $\varepsilon_s = 4.52$ for AQON and $\varepsilon_0 = 3.81$, $\varepsilon_s = 4.72$ for AQOF). These calculations assume a relatively sparse surface coverage (2.5 molecules/nm^2), meaning that even higher dielectric constants should be attainable with higher surface density.

Interestingly, leakage currents through these materials are also substantially reduced in comparison to the AQ material. Near the Fermi energy, we find conductance values of 27.8 nS for AQON and 64.9 nS for AQOF molecules, corresponding to monolayer current densities of 20.7 and 68.6 nA/nm^2 at 0.25 V

and transport reductions relative to the AQ material of ~2.7 and ~2.2 orders of magnitude, respectively. We believe that these reductions are a consequence of the broken electrode−molecule bonding symmetry caused by the substituent groups and their interaction with Au atoms in the electrodes, and the localization of the HOMO on the donor substituted fragment. These results serve as a proof of concept, showing that the dielectric response and charge transport of thin film materials can be simultaneously designed in the coherent regime to meet requirements for specific applications.

CONCLUSIONS

We investigated the relationship between charge transport and dielectric response in the quantum coherent regime, finding that the two can be nearly independent in certain systems. As an example, we first compared the properties of a cross-conjugated AQ material to a linear-conjugated AC material. Despite a ~50-fold reduction in the room-temperature conductance of the cross-conjugated molecule, caused by destructive quantum interference of the electronic excitations in the system, the dielectric behavior of the materials is nearly indistinguishable. Although these calculations contradict the established trend in conventional bulk semiconductors, where polarizability and mobility are inversely proportional to the gap energy,[5−8] at the nanoscale quantum coherence influences these observables differently. To highlight the importance of this point, we suggested two materials based on the AQ molecule which exhibit large dielectric constants (~4.5) while maintaining the interference-induced reduction in the conductance.

Quantum interference effects are ubiquitous in molecular systems and can often be controlled by chemical design. In the examples considered here, we have shown that coherence is an important resource which can be utilized in molecular materials to help circumvent certain design challenges. Our hope is that this work will motivate the use of quantum coherence in the development of future dielectric materials.

METHODS

Quantum Transport. In devices composed of small conjugated organic molecules operating near room temperature, the current is predominantly quantum coherent and elastic, and may be calculated as[31]

$$I(\Delta V) = \frac{2e}{h}\int_{-\infty}^{+\infty} Tr\{t(E)t^{\dagger}(E)\}\left[f\left(E,\mu+\frac{e\Delta V}{2}\right)-f\left(E,\mu-\frac{e\Delta V}{2}\right)\right]dE \tag{1.6}$$

where $f(E) = (\exp([E-\mu]/kT)+1)^{-1}$ are the Fermi distributions of the electrodes, $t(E)$ is the transmission amplitude, ΔV is the bias applied between left and right electrodes, μ is the chemical potential of the electrodes, and E is the incident energy. In the linear-response regime, where the temperature and the bias applied across the device are small compared to the operating temperature and chemical potential of the electrodes, respectively, the differential conductance may be expressed as

$$\frac{dI}{dV} = G_0\int dE\left(-\frac{\partial f_0}{\partial E}\right)Tr\{t(E)t^{\dagger}(E)\} \tag{1.7}$$

where $f_0(E)$ is the Fermi function of the electrodes without any applied bias or temperature difference.

Within the nonequilibrium Green's function (NEGF) framework, the transmission amplitudes can be expressed in terms of the junction's retarded Green's function (*cf.* eq 1.5 in the main text).[15,32] Within this framework, the molecular junction is decomposed into three parts: the left and right electrodes and the central scattering region, a system interacting with the electrodes and including the molecule and a few metallic screening layers. We solve the electronic structure problem of each of these parts at the Kohn−Sham Density Functional Theory (KS-DFT) level and construct the junction's Green's function using

$$G(E) = [\mathbf{S}E - H_{KS} - \Sigma_L(E) - \Sigma_R(E)]^{-1} \tag{1.8}$$

where $\mathbf{S}$ is the overlap matrix, H_{KS} is the Kohn−Sham Hamiltonian, and $\Sigma_{L,R}$ are the self-energies which describe the influence of coupling macroscopic electrodes to the central scattering region. We treat these macroscopic electrodes as infinite periodic bulks. Their electronic structures and Green's function are computed from KS-DFT and connected to the central scattering region through the self-energy terms.

To create the scattering region, we started by optimizing the geometries of the isolated molecules at the DFT/B3LYP level[46,47] and using a 6-31G** Gaussian basis set as implemented in the NWchem-6.3 package.[48] We then contacted the optimized molecules to two Au(111) surfaces with the sulfur atoms lying atop a gold atom on each side as a contact geometry. The Au−S bond distance was taken to be 2.42 Å. Finally, we restrict the scattering region to the molecule and 5 gold layers on each side, which allows for a good convergence of the transport properties.

The NEGF-DFT and transmission computations are done using the implementation of the ATK2008.10 package.[49,50] We use the GGA.revPBE exchange-correlation[51,52] functional for consistency with the dielectric properties computations, a DoubleZeta+Polarization numerical basis set[53] for electrons in molecular atoms, a SingleZeta+Polarization numerical basis set for electrons in gold atoms and a (7,7,50) Monkhorst−Pack k-sampling. This set of parameters has been carefully checked to ensure the convergence of the transmission spectrum. Although KS-DFT tends to overestimate the conductance and Fermi-level pinning effects,[40] it has been shown to characterize the chemical trends and transport ratios in the systems we consider here.[18]

Dielectric Response. The dielectric constants for monolayer films are calculated using a finite difference approach developed in a previous work.[3] To begin, a single molecule is placed in a periodic unit cell of dimensions x, y, and z. The x and y dimensions correspond to surface coverage of the molecular monolayer. Surface density values typically range from 2.0 to 5.0 molecules/nm^2, depending on the interaction between substrate and assembled monolayer. In this work, we consider a surface coverage of 2.5 molecules/nm^2, with x and y dimensions of 4.5 and 8.8 Å, respectively. The z-axis lies perpendicular to the surface and is long enough to ensure at least 15.0 Å of vacuum between monolayers, where image effects are negligible. After optimizing geometry of the molecular film, two different electric fields, E_1 and E_2, are applied separately and geometry is optimized in the presence of the electric field. E_{ext} is defined as the difference between E_1 and E_2. For all dielectric simulations, $E_1 = 5.14 \times 10^8$ V/m and $E_2 = -5.14 \times 10^8$ V/m, typical values for applied electric fields in devices.[18]

Electric fields are applied parallel to the *z*-axis, simulating an electric field across a monolayer.

After applying the two electric fields, the change in dipole moment is used to determine the dielectric constant *via*[26]

$$\varepsilon = \frac{\varepsilon_0 E_{ext}}{\varepsilon_0 E_{ext} - \Pi} \quad (1.9)$$

where ε_0 is the vacuum permittivity. The polarization for the monolayer is defined as

$$\Pi = \frac{\Delta\mu}{V_{ML}} \quad (1.10)$$

where $\Delta\mu$ is the change in dipole moment of the monolayer induced by an applied field and V_{ML} is the volume of the monolayer. V_{ML} is the area of the unit cell times the thickness of the monolayer. It has been shown that, in certain cases, the interactions between substrate and organic monolayer can have little effect on dielectric response, allowing us to forgo implementing explicit surfaces.[54]

We determine two different dielectric constants, the optical dielectric constant, ε_o, represents dielectric responses at high frequency (*i.e.*, as $\omega \rightarrow \infty$) before any geometry changes occur in the presence of the electric field. Static dielectric constant, ε_s, represents dielectric responses at low frequency (*i.e.*, as $\omega \rightarrow 0$) after geometry optimization. In both the optical and static response, no molecular translational or rotational motion is allowed.

Dielectric calculations are performed in QUANTUMESPRESSO.[55] Two different density functionals are applied in these studies. Generalized Gradient Approximation (GGA) as implemented by the Perdew–Burke–Ernzerhof (PBE)[51] is used to treat all systems. Heyd–Scuseria–Ernzerhof (HSE),[54] a screened hybrid density functional, is used on smaller molecules to verify the accuracy of our results. It is not applied to all systems due to its large computational expense within planewave packages. For PBE functionals, Vanderbilt ultrasoft pseudopotentials[35] are used with kinetic energy cutoff values of 60 and 660 Ry for wave functions and charge density, respectively. Forces were converged to 20 meV/Å and a k-point scheme of $2 \times 2 \times 1$ was implemented.

Conflict of Interest: The authors declare no competing financial interest.

Acknowledgment. The research was partially supported by the MRSEC program of NSF (DMR-1121262) through the Northwestern University Materials Research Center. J.P.B., C.V. D., and M.A.R. were supported by Center for Bio-inspired Energy Science, an Energy Frontier Research Center funded by the U.S. Department of Energy, Office of Science, Basic Energy Sciences under Award No. DE-SC0000989. C.V.D. was also supported by a Gustave Boël - Sofina Fellowship of the Belgian American Educational Foundation (BAEF). C.V.D. acknowledges the Laboratory for Chemistry of Novel Materials at the Université de Mons in Belgium for their computational support and resources.

REFERENCES AND NOTES

1. International Technology Roadmap for Semiconductors: 2013 Edition. http://public.itrs.net.
2. Facchetti, A.; Yoon, M. H.; Marks, T. J. Gate Dielectrics for Organic Field Effect Transistors: New Opportunities for Organic Electronics. *Adv. Mater.* **2005**, *17*, 1705–1725.
3. Heitzer, H. M.; Marks, T. J.; Ratner, M. A. First-Principles Calculation of Dielectric Response in Molecule-Based Materials. *J. Am. Chem. Soc.* **2013**, *135*, 9753–9759.
4. Marks, T. J. Materials for Organic and Hybrid Inorganic/Organic Electronics. *MRS Bull.* **2010**, *35*, 1018–1027.
5. Brothers, E. N.; Scuseria, G. E.; Kudin, K. N. Longitudinal Polarizability of Carbon Nanotubes. *J. Phys. Chem. B* **2006**, *110*, 12860–12864.
6. Sonmez, G.; Meng, H.; Wudl, F. Very Stable Low Band Gap Polymer for Charge Storage Purposes and Near-Infrared Applications. *Chem. Mater.* **2003**, *15*, 4923–4929.
7. Yu, Y. H.; Lee, S. C.; Yang, C. S.; Choi, C. K.; Jung, W. K. Mobility, Energy Gap and Dielectric Constant in Sioc Films. *J. Korean Chem. Soc.* **2003**, *42*, 682–685.
8. Penn, D. R. Wave-Number-Dependent Dielectric Function of Semiconductors. *Phys. Rev.* **1962**, *128*, 2093.
9. Markussen, T.; Thygesen, K. S. Temperature Effects on Quantum Interference in Molecular Junctions. *Phys. Rev. B* **2014**, *89*, 085420–085420.
10. Kocherzhenko, A.; Siebbeles, L. D.; Grozema, F. C. Charge Transfer through Molecules with Multiple Pathways: Quantum Interference and Dephasing. *J. Phys. Chem. C* **2010**, *114*, 7973–7979.
11. Baer, R.; Neuhauser, D. Phase Coherent Electronics: A Molecular Switch Based on Quantum Interference. *J. Am. Chem. Soc.* **2002**, *124*, 4200–4201.
12. Markussen, T.; Stadler, R.; Thygesen, K. S. The Relation between Structure and Quantum Interference in Single Molecule Junctions. *Nano Lett.* **2010**, *10*, 4260–4265.
13. Sautet, P.; Joachim, C. Electronic Interference Produced by a Benzene Embedded in a Polyacetylene Chain. *Chem. Phys. Lett.* **1988**, *153*, 511–516.
14. Hansen, T.; Solomon, G. C.; Andrews, D. Q.; Ratner, M. Interfering Pathways in Benzene: An Analytical Treatment. *J. Chem. Phys.* **2009**, *131*, 194704–194704.
15. Bergfield, J. P.; Jacquod, P.; Stafford, C. A. Coherent Destruction of Coulomb Blockade Peaks in Molecular Junctions. *Phys. Rev. B* **2010**, *82*, 205405.
16. Aradhya, S. V.; Meisner, J. S.; Krikorian, M.; Ahn, S.; Parameswaran, R.; Steigerwald, M. L.; Nuckolls, C.; Venkataraman, L. Dissecting Contact Mechanics from Quantum Interference in Single-Molecule Junctions of Stilbene Derivatives. *Nano Lett.* **2012**, *12*, 1643–1647.
17. Cardamone, D. M.; Stafford, C. A.; Mazumdar, S. Controlling Quantum Transport through a Single Molecule. *Nano Lett.* **2006**, *6*, 2422–2426.
18. Guedon, C. M.; Valkenier, H.; Markussen, T.; Thygesen, K. S.; Hummelen, J. C.; van der Molen, S. J. Observation of Quantum Interference in Molecular Charge Transport. *Nat. Nanotechnol.* **2012**, *7*, 305–309.
19. Bergfield, J. P.; Solomon, G. C.; Stafford, C. a.; Ratner, M. a. Novel Quantum Interference Effects in Transport through Molecular Radicals. *Nano Lett.* **2011**, *11*, 2759–2764.
20. Solomon, G. C.; Andrews, D. Q.; Goldsmith, R. H.; Hansen, T.; Wasielewski, M. R.; Van Duyne, R. P.; Ratner, M. A. Quantum Interference in Acyclic Systems: Conductance of Cross-Conjugated Molecules. *J. Am. Chem. Soc.* **2008**, *130*, 17301–17308.
21. Ke, S.-H.; Yang, W.; Baranger, H. U. Quantum-Interference-Controlled Molecular Electronics. *Nano Lett.* **2008**, *8*, 3257–3261.
22. Bergfield, J. P.; Stafford, C. A. Thermoelectric Signatures of Coherent Transport in Single-Molecule Heterojunctions. *Nano Lett.* **2009**, *9*, 3072–3067.
23. Sautet, P.; Joachim, C. Are Electronic Interference Effects Important for STM Imaging of Substrates and Adsorbates?: A Theoretical Analysis. *Ultramicroscopy* **1992**, *44*, 115–121.
24. Ballmann, S.; Hartle, R.; Coto, P.; Elbing, M.; Mayor, M.; Bryce, M.; Thoss, M.; Weber, H. Experimental Evidence for Quantum Interference and Vibrationally Induced Decoherence in Single-Molecule Junctions. *Phys. Rev. Lett.* **2012**, *109*, 1–5.
25. Datta, S. *Electronic Transport in Mesoscopic Systems*; Cambridge University Press: Cambridge, U.K., 1995.
26. Mahan, G. D. *Many-Particle Physics*; Plenum Press: New York, 1990.
27. Negele, J. W.; Orland, H. *Quantum Many-Particle Systems*; Advanced Book Classics; Addison-Wesley Pub. Co.: Redwood City, CA, 1998; pp 474–474.
28. Mattuck, R. D. *A Guide to Feynman Diagrams in the Many-Body Problem*; Dover Publications, Inc.: New York, 1992.
29. Bruus, H.; Flensberg, K. *Many-Body Quantum Theory in Condensed Matter Physics: An Introduction*; Oxford University Press: Oxford , U.K., 2002.
30. Buttiker, M. Four-Terminal Phase-Coherent Conductance. *Phys. Rev. Lett.* **1986**, *57*, 1761.

31. Imry, Y.; Landauer, R. Conductance Viewed as Transmission. *Rev. Mod. Phys.* **1999**, *71*, S306–S312.
32. Fisher, D. S.; Lee, P. A. Relation between Conductivity and Transmission Matrix. *Phys. Rev. B* **1981**, *23*, 6851–6854.
33. Yeyati, A. L.; Buttiker, M. Scattering Phases in Quantum Dots: An Analysis Based on Lattice Models. *Phys. Rev. B* **2000**, *62*, 7307.
34. Brandbyge, M.; Tsukada, M. Local Density of States from Transmission Amplitudes in Multichannel Systems. *Phys. Rev. B* **1998**, *57*, R15088.
35. Taniguchi, T.; Buttiker, M. Friedel Phases and Phases of Transmission Amplitudes in Quantum Scattering Systems. *Phys. Rev. B* **1999**, *60*, 13814–13823.
36. Phelan, N. F.; Orchin, M. Cross Conjugation. *J. Chem. Educ.* **1968**, *45*, 633.
37. Limacher, P. A.; Luthi, H. P. Cross-Conjugation. *Wiley Interdiscip. Rev.: Comput. Mol. Sci.* **2011**, *1*, 477–486.
38. Solomon, G. C.; Bergfield, J. P.; Stafford, C. A.; Ratner, M. A. When "Small" Terms Matter: Coupled Interference Features in the Transport Properties of Cross-Conjugated Molecules. *Beilstein J. Nanotechnol.* **2011**, *2*, 862–871.
39. Solomon, G. C.; Andrews, D. Q.; Van Duyne, R. P.; Ratner, M. A. Electron Transport through Conjugated Molecules: When the Pi-System Only Tells Part of the Story. *ChemPhysChem* **2009**, *10*, 257–264.
40. Van Dyck, C.; Geskin, V.; Cornil, J. Fermi Level Pinning and Orbital Polarization Effects in Molecular Junctions: The Role of Metal Induced Gap States. *Adv. Funct. Mater.* **2014**, *24*, 6154–6165.
41. Kim, B.; Ho Choi, S.; Zhu, X.-Y.; Frisbie, D. C. Molecular Tunnel Junctions Based on Pi-Conjugated Oligoacene Thiols and Dithiols between Ag, Au, and Pt Contacts: Effect of Surface Linking Group and Metal Work Function. *J. Am. Chem. Soc.* **2011**, *49*, 19864–19877.
42. Kanis, D. R.; Ratner, M. A.; Marks, T. J. Design and Construction of Molecular Assemblies with Large Second-Order Optical Nonlinearities. Quantum Chemical Aspects. *Chem. Rev.* **1994**, *94*, 195–242.
43. Brown, E. C.; Marks, T. J.; Ratner, M. A. Nonlinear Response Properties of Ultralarge Hyperpolarizability Twisted Pi-System Donor-Acceptor Chromophores. Dramatic Environmental Effects on Response. *J. Phys. Chem. B* **2008**, *112*, 44–50.
44. Nitzan, A. Electron Transmission through Molecules and Molecular Interfaces. *Annu. Rev. Phys. Chem.* **2001**, *52*, 681–750.
45. Nitzan, A.; Ratner, M. A. Electron Transport in Molecular Wire Junctions. *Science* **2003**, *300*, 1384–1389.
46. Becke, A. D. Density Functional Thermochemistry. III. The Role of Exact Exchange. *J. Chem. Phys.* **1993**, *98*, 5648–5652.
47. Lee, C.; Yang, W.; Parr, R. G. Development of the Colle-Salvetti Correlation-Energy Formula into a Functional of the Electron Density. *Phys. Rev. B* **1988**, *37*, 785–789.
48. Valiev, M.; Bylaska, E. J.; Govind, N.; Kowalski, K.; Straatsma, T. P.; Van Dam, H. J. J.; Wang, D.; Nieplocha, J.; Apra, E.; Windus, T. L.; et al. Nwchem: A Comprehensive and Scalable Open-Source Solution for Large Scale Molecular Simulations. *Comput. Phys. Commun.* **2010**, *181*, 1477–1489.
49. Taylor, J.; Guo, H.; Wang, J. *Ab Initio* Modeling of Quantum Transport Properties of Molecular Electronic Devices. *Phys. Rev. B* **2001**, *63*, 245407.
50. Brandbyge, M.; Mozos, J.-L.; Ordejon, P.; Taylor, J.; Stokbro, K. Density-Functional Method for Nonequilibrium Electron Transport. *Phys. Rev. B* **2002**, *65*, 165401.
51. Perdew, J. P.; Burke, K.; Ernzerhof, M. Generalized Gradient Approximation Made Simple. *Phys. Rev. Lett.* **1996**, *77*, 3865–3868.
52. Zhang, Y.; Yang, W. Comment on a Generalized Gradient Approximation Made Simple. *Phys. Rev. Lett.* **1998**, *80*, 890–890.
53. Junquera, J.; Paz, O.; Sanchez-Portal, D.; Artacho, E. Numerical Atomic Orbitals for Linear-Scaling Calculations. *Phys. Rev. B* **2001**, *64*, 235111.
54. Yu, L.; Ranjan, V.; Nardelli, M. B.; Bernholc, J. First-Principles Investigations of the Dielectric Properties of Polypropylene/Metal-Oxide Interfaces. *Phys. Rev. B* **2009**, *80*, 165432.
55. Giannozzi, P.; Baroni, S.; Bonini, N.; Calandra, M.; Car, R.; Cavazzoni, C.; Ceresoli, D.; Chiarotti, G. L.; Cococcioni, M.; Dabo, I. Quantum Espresso: A Modular and Open-Source Software Project for Quantum Simulations of Materials. *J. Phys.: Condens. Matter* **2009**, *21*, 395502.